BIOCHEMISTRY
including biophysical chemistry & molecular biology

ARTICLE

pubs.acs.org/biochemistry

RapA, *Escherichia coli* RNA Polymerase SWI/SNF Subunit-Dependent Polyadenylation of RNA

Michael Richmond, Raghavendra R. Pasupula, Seema G. Kansara, Joshua P. Autery, Brent M. Monk, and Maxim V. Sukhodolets*

Department of Chemistry and Biochemistry, Lamar University, Beaumont, Texas 77710, United States

Supporting Information

ABSTRACT: In this work, we describe RapA-dependent polyadenylation of model RNA substrates and endogenous, RNA polymerase-associated nucleic acid fragments. We demonstrate that the *Escherichia coli* RNA polymerase obtained through the classic purification procedure carries endogenous RNA oligonucleotides, which, in the presence of ATP, are polyriboadenylated in a RapA-dependent manner by an accessory poly(rA) polymerase. RNA polymerase isolated from poly(A) polymerase- (PAP-) and polynucleotide phosphorylase- (PNP-) deficient *E. coli* strain lacks accessory $(rA)_n$-synthetic activity. Experiments with reconstituted RNA polymerase−PAP and RNA polymerase−PNP mixtures suggest that RapA enables the polyadenylation by PAP of RNA polymerase-associated RNA. Mutations disrupting RapA's ATP-hydrolytic function disrupt RapA-dependent polyadenylation, and the *rapA*$^-$ *E. coli* strain displays a measurable reduction in RNA polyadenylation. RapA-dependent polyadenylation can also be modulated by mutations in the section of RapA's SWI/SNF domain linked to interaction with single-stranded nucleic acid. We have developed enzymatic assays in which model, synthetic RNAs are polyriboadenylated in a RapA-dependent manner. Taken together, our results are consistent with RapA acting as an RNA polymerase-associated, ATP-dependent RNA translocase. Our work further links RapA to RNA remodeling and provides new mechanistic insights into the functional interaction between RNA polymerase and RapA.

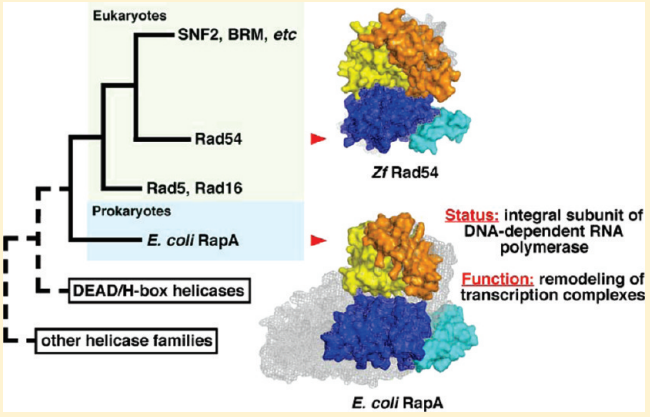

The helicase-like SWI/SNF proteins are found in organisms belonging to distant kingdoms, from bacteria to humans, indicating that they perform a very basic, yet not fully understood function. Four out of six characteristic homology motifs present in SWI/SNF proteins are found in DEAD/H family of DNA and RNA helicases, the class of enzymes capable of translocation on single-stranded nucleic acids in an ATP-dependent manner. Studies with eukaryotic SWI/SNF proteins indicated that they could detach DNA from histones and other bound proteins. This led to views that they function to provide direct access to DNA during diverse cellular processes such as transcription, replication, DNA repair, and recombination. When the SWI/SNF protein family was originally introduced as a derivative of the DEAD/H helicase family[1,2] (also Figure 1), it was apparent that it is an ancient and ubiquitous class of proteins, since the homology analyses predicted the existence of both eukaryotic and prokaryotic members, the latter not known at the time. The first prokaryotic SWI/SNF protein, RapA, has been identified within a few years after publication of these seminal comparative studies, perhaps unexpectedly, as a subunit of DNA-dependent RNA polymerase.[3] *In vivo* studies have demonstrated that the deletion of the *rapA* gene yielded little or no effect on cell growth, mutation rates, and UV sensitivity[4] [initial report of UV sensitivity associated with *rapA* mutation[5] was later attributed to an artifact[4] (presence of a phage whose lytic stage was triggered by a UV irradiation)] under a variety of experimental conditions. Yet, *rapA* mutation resulted in a unique phenotype, rendering bacteria incapable of efficient growth on agar plates in high salt.[6,7] *In vitro*, RapA enhanced multiround transcription in a salt concentration-specific manner.[6,8] Studies targeting individual stages of the transcription cycle yielded evidence of RapA promoting RNA displacement from RNA polymerase−RNA[7,9] and noncanonical ssRNA−dsDNA complexes (putative triplexes), which are stabilized in high salt.[9] The latter evidence led to a hypothesis that remodeling of noncanonical ssRNA−dsDNA complexes could be a function shared by RapA homologues; such a function would be in accord with RapA's status as an accessory subunit of DNA-dependent RNA polymerase.

In this work, we describe RapA-dependent polyadenylation of model RNA substrates and endogenous, RNA polymerase-associated nucleic acid fragments. We demonstrate that $(rA)_n$-synthetic activity copurifies with native RapA−RNA polymerase

Received: June 24, 2010
Revised: February 4, 2011
Published: February 07, 2011

dx.doi.org/10.1021/bi101017x | *Biochemistry* 2011, 50, 2298–2312

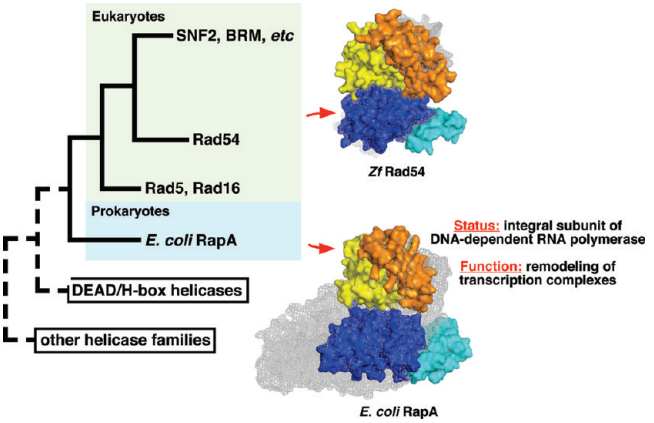

Figure 1. Structural homology between prokaryotic and eukaryotic SWI/SNF proteins. A dendrogram illustrating the origin of SWI/SNF proteins. The dendrogram, reminiscent to that originally reported by Kolstø *et al.*[2] and incorporating elements from a detailed SWI/SNF family tree reported by Eisen *et al.*,[22] is updated with RapA's structure,[10] cellular status,[3−6] and functions.[6,7,9] The structure of the Zebrafish Rad54 homologue[21] is also shown. The homologous domains in the two proteins are shown in colors matching those in the work by Shaw *et al.*[10] The domain harboring signature SWI/SNF motifs (referred to below as SWI/SNF domain) is shown in orange and yellow.

complexes. We analyzed the origin and mechanistic aspects of this enzymatic activity and concluded that the endogenous, RNA polymerase-associated RNA oligonucleotides (which have been known to copurify with the *Escherichia coli* RNA polymerase and whose presence we have further confirmed through mass spectrometry analyses) are polyadenylated in a RapA-dependent manner by an accessory poly(A) polymerase (PAP). We describe a modulation of this activity by two dissimilar classes of mutations within RapA's SWI/SNF domain and demonstrate that the *rapA*$^{-}$ *E. coli* strain displays a measurable reduction in RNA polyadenylation. We mimic the observed activity in reconstituted RapA−RNA polymerase−(purified) PAP mixtures and show that model, synthetic RNAs can be polyadenylated in a RapA-dependent manner. This work further links the function of RapA to RNA remodeling and provides new mechanistic insights into the functional interaction between RNA polymerase and RapA.

MATERIALS AND METHODS

Enzymes. The *E. coli* RNA polymerase was isolated as previously described,[19] with modifications described in ref 7. The purification procedure (a derivative of the protocol developed by the Burgess group),[11] which yields native *E. coli* RNA polymerase complexes (the core RNA polymerase, the RNA polymerase holoenzyme, and the RapA−holoenzyme complex),[3,8] is summarized in Figure 4. Recombinant (His-tagged) RapA[9] was isolated as previously described;[7] the purification procedure is also described below (see Figure 10B). *E. coli* poly(A) polymerase (PAP; also referred to as PAP I)[20] and RNase-free DNase I were obtained from New England Biolabs (respectively no. M0276, 5 units/μL, and no. M0303, 2 units/μL). Purified *E. coli* polynucleotide phosphorylase (PNP) was obtained from Sigma-Aldrich (no. N9664). DNase-free RNase was a product of Boehringer (no. 119915; 2 units/μL); RNase I_f was obtained from New England Biolabs (no. M0243; 50 units/μL). Calf intestinal alkaline phosphatase was obtained from Invitrogen (no. 18009-019; 20 units/μL).

Synthetic RNA and DNA Probes. Synthetic RNA oligonucleotides were purchased from Dharmacon/Invitrogen; DNA oligonucleotides were purchased from Invitrogen. Oligonucleotides were either cartridge- or gel-purified, as previously described.[9]

Polyadenylation Assays. Polyadenylation reactions were carried out in either buffer C (50 mM Tris-HCl, 10 mM $MgCl_2$, 100 mM NaCl, 1 mM dithiothreithol, pH 7.9) or buffer D (20 mM Tris−acetate, 10 mM magnesium acetate, 50 mM potassium acetate, 1 mM dithiothreithol, pH 7.9); the reaction buffers are specified in the figure legends. Before each experiment, purified enzymes [stored as 3−6 mg/mL glycerol stocks in 1× TGED (10 mM Tris-HCl, 0.1 mM EDTA, 0.1 mM dithiothreithol, 5% glycerol, pH 7.5) containing 50% glycerol] were diluted with ultrapure water (KD Medical, no. RGF-3410), typically to 0.4−1 mg/mL to obtain "working solutions" (which were stored on ice for the duration of an experiment). A typical 20 μL extension reaction contained 2 μL of 10× reaction buffer C, purified enzymes at 0.1−1 μM (the enzymes' concentrations are specified in the figure legends), and ultrapure water to the final volume of 16 μL. The RNA synthesis was initiated by the addition of 4 μL of 5 mM ATP (unless indicated otherwise in the figure legends) containing [α-^{32}P]ATP (MP Biomedicals, no. 32007U). In [α-^{32}P]ATP (as obtained from the vendor) the content of [α-^{32}P]ADP (determined after TLC chromatography on PEI-cellulose plates) was consistently <0.15%; ^{32}P-labeled nucleoside triphosphates other than ATP [which show dissimilar mobilities in PEI-cellulose chromatography (for example, see ref 19)] were nondetectable. Reaction mixtures were incubated for 30 min at 37 °C unless indicated otherwise in the figure legends. In some of the experiments, following the incubation, the reaction products were treated with a nuclease (either RNase or DNase); the nuclease treatment is described in the figure legends. Typically, when the extension products were analyzed on denaturing polyacrylamide gels, DNase-free RNase (Boehringer) was used to produce complete ladders of ^{32}P-labeled nucleic acid fragments (as seen in Figures 3A, 4B, and 8C). The reactions were terminated by the addition of an equal volume of stop solution (50% glycerol, 50 mM EDTA, 0.1% bromphenol blue, pH 7.5); reaction mixtures were denatured by boiling and the ^{32}P-labeled RNAs/nucleotides fractionated by either denaturing PAGE or TLC chromatography on PEI-cellulose plates, as described below.

Denaturing PAGE. Denaturing polyacrylamide gels were cast using the SequaGel kit (National Diagnostics); the polyacrylamide concentrations are specified in the figure legends. Gibco BRL model SA gel apparatuses with custom-manufactured borosilicate glass plates (short plate size: 195 mm × 337 mm) and 0.4 mm spacers were used. Gels were typically run at 25−35 W using 0.5× TBE as a running buffer; the TBE solution was obtained as a 10× stock at KD Medical (no. RGF-3330). After electrophoresis, X-ray films were exposed to "wet" gels covered with plastic wrap, typically for 8−48 h at −80 °C with Kodak BioMax MS intensifying screens. The images of the developed X-ray films were captured with an Olympus model C-5060 wide zoom digital camera over a white light box (the gel images shown in this work did not undergo brightness/contrast adjustments, sharpening, or any other form of digital enhancement); typical exposure settings were 1/80−1/200. Data were quantitated, plotted, and analyzed as previously described.[7]

Nucleic acid detection assays with RiboGreen (RG) (Invitrogen/Molecular Probes, no. R11491) or SYBR II (Sigma-Aldrich,

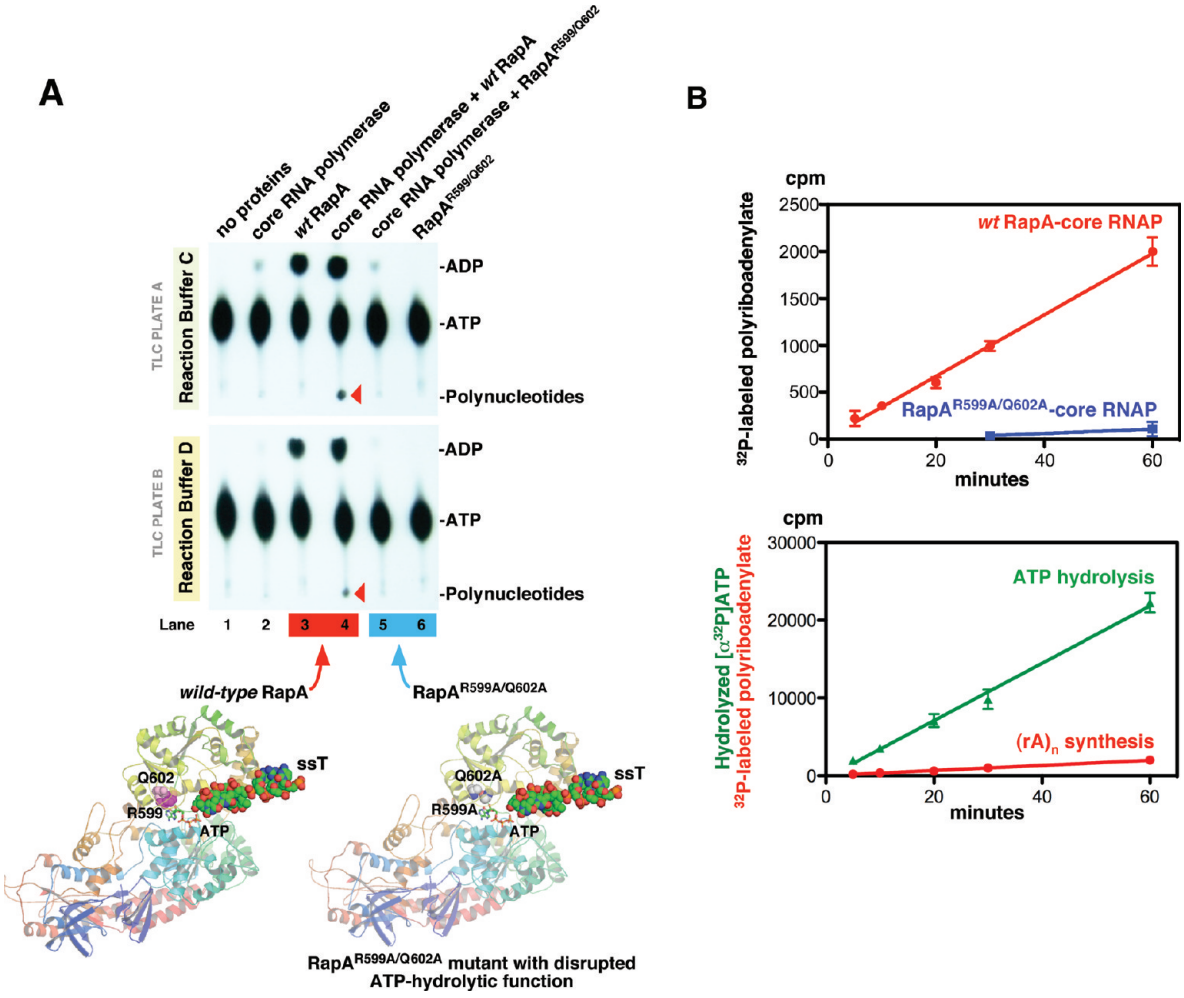

Figure 2. Synthesis of polyriboadenylate in RapA−core RNA polymerase−ATP mixtures. Poly(rA)-synthetic activity was assayed as described in Materials and Methods; the reaction buffers are indicated in each panel. (A) ATP hydrolysis and polyriboadenylate synthesis in RapA−core RNA polymerase−ATP mixtures. Following a 30 min incubation at 37 °C, reaction products were fractionated by thin-layer chromatography on PEI-cellulose plates, as described in Materials and Methods; ingredients of individual reactions are indicated at the top. Core RNA polymerase, 0.53 μM; wild-type RapA, 0.5 μM; RapA$^{R599A/Q602A}$, 0.58 μM; [α-^{32}P]ATP, 1 mM. On each TLC plate, the positions of ^{32}P-labeled ATP, ADP, and polynucleotides (remaining at the origin of the plate) are indicated. The structures of RapA−ATP−ssT complexes[7] are shown at the bottom. (B) Top panel: Kinetics of polyriboadenylate synthesis in wild-type RapA−core RNA polymerase−ATP and RapA$^{R599A/Q602A}$−core RNA polymerase−ATP mixtures. Quantitated results of two independent experiments, similar to that described in panel A, lanes 4 and 5 (top panel, reaction buffer C), are shown. The kinetics of polyriboadenylate synthesis (red circles) and ATP hydrolysis (green triangles) in the same reactions are shown in the bottom panel.

no. S9305) were carried out in either 384-well or 96-well black plates (Greiner) using a Fluoroscan Ascent FL fluorometer (Thermo-Fisher Scientific). For RNA quantitation assays, RG or SYBR II was diluted 1000−4000-fold with 1× buffer C to make a 2× dye stock. Equal volumes of thus made dye solution and a test sample were mixed in a well of a plate. With 384-well plates, the total reaction volume was 20 μL; with 96-well plates, reaction volumes were 100−120 μL. With both dyes, 485 nm/538 nm (excitation/emission) filter pairs were used; typical integration times were 400−1000 ms. Fluorescence intensity in the samples was determined at ambient temperature (21−22 °C). In the presence of RNA polymerase−(endogenous) oligonucleotide complexes, fluorescence intensity of either dye typically increased 60−300-fold [compared to 1.2−4-fold effects seen in the presence of excess control proteins (BSA, lysozyme, thyroglobulin)]. Key experiments were carried out with RiboGreen; changes in fluorescence observed with SYBR II generally mimicked those seen with RG.

ATPase activity assays were carried out as previously described.[3,7]

Mutagenesis. The QuickChange site-directed mutagenesis kit (Stratagene) was used to construct the described RapA mutations. Primers MS905R (3′-ATTAAAGTCTCCGGCATTAT-GGGCGCAGAGGACGGTACCCGAGAACCCGGAGCG-TATTTT-5′) and MS906R (antiparallel to MS905R) were used to construct the *rapA** mutation (R457E, K458D, S459G, A460T, E461R, R465D). After amplification with mutagenic primers and *Dpn*I digestion of pQE32-RapA[9] template DNA, aliquots of the reaction mixtures were used to transform M15/pRep4 *E. coli* competent cells. Plasmid DNAs from individual clones were purified and analyzed. The expression of full-length (mutant) RapA in individual clones was verified by SDS−PAGE−Western blot using RapA-specific

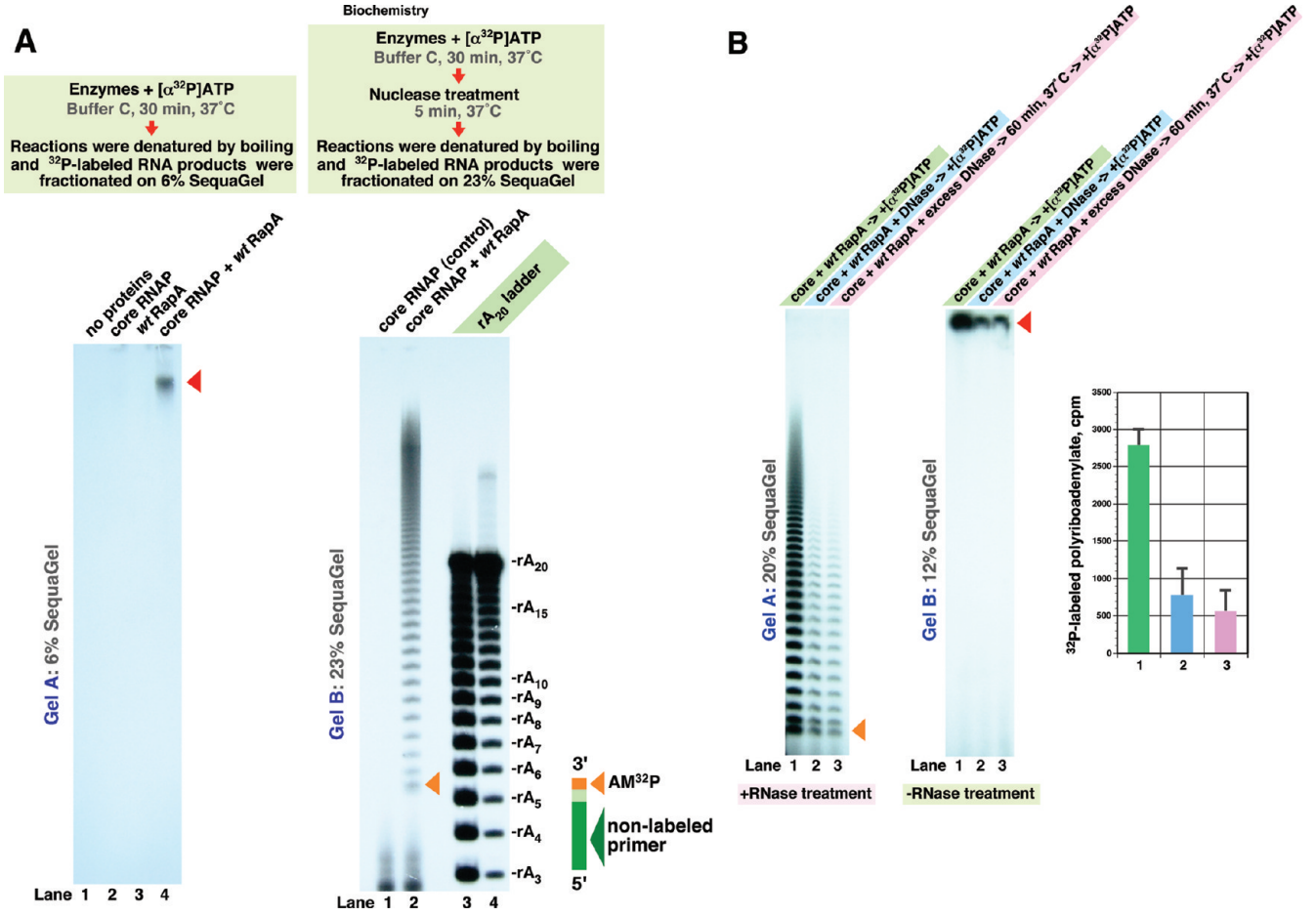

Figure 3. DNA-independent extension of the endogenous, protein-associated oligonucleotide(s) in RapA−core RNA polymerase−ATP mixtures. (A) Polyadenylation of endogenous oligonucleotide(s) in RapA−core RNA polymerase−ATP mixtures. Reactions were carried out in reaction buffer C, as described in Materials and Methods; schematics of the experiments are shown at the top. Core RNA polymerase, 0.53 μM; wild-type RapA, 0.5 μM; [α-^{32}P]ATP, 1 mM. Gel A: reaction mixtures were incubated for 30 min at 37 °C. Following the addition of an equal volume of stop solution (50% glycerol, 50 mM EDTA, 0.1% bromphenol blue, pH 7.5), the reaction mixtures were denatured by boiling, and ^{32}P-labeled reaction products were fractionated on 6% SequaGel. Gel B, lanes 1 and 2: like lanes 3 and 4 in gel A, except that after a 30 min incubation at 37 °C the reactions were treated with 1 unit of DNase-free RNase/10 μL reaction for 5 min at room temperature, and ^{32}P-labeled reaction products were fractionated on 23% SequaGel. Size markers [^{32}P-labeled $(rA)_{20}$ (Dharmacon) treated with DNase-free RNase as described above] are in lanes 3 and 4. In gel B, orange arrowheads indicate the shortest ^{32}P-labeled extension product. (B) The $(rA)_n$-synthetic reaction in question is DNA-independent. Gel B, lane 1: similar to lane 4 in panel A (gel A). Gel B, lane 2: similar to lane 1, except that the (10 μL) reaction mixture contained 1 unit of RNase-free DNase. Gel B, lane 3: similar to lane 1, except that the RapA−core RNA polymerase mixture (in buffer C) was preincubated for 60 min with 2 units of RNase-free DNase before the addition of ATP. Reaction mixtures in lanes 1−3 in gel A were similar to those in gel B, except that this set of samples was treated with DNase-free RNase, as described in panel A. The quantitated levels of total RNA are shown at the right.

antibodies.[3,4] The mutant His-tagged RapA protein was overproduced and purified as previously described for wild-type (His-tagged) RapA.[7]

***In vivo* ^{32}P labeling of nucleic acids** is described in Supporting Information.

***E. coli* Strains.** The PAP I$^-$ PNP$^-$ *E. coli* strain[23] was obtained from S. R. Kushner; the previously constructed MG1655*rapA*$^-$ *E. coli* strain[4] was also used in this work.

RESULTS

$(rA)_n$-Synthetic Activity Is Associated with the RapA−RNA Polymerase Complex. To date, the effects of RapA in *in vitro* transcription have been studied almost exclusively with RNA polymerase holoenzyme. However, it was established that the core RNA polymerase is the primary RapA-interacting species in *E. coli*.[4,10] We therefore reinvestigated the effects of RapA on transcriptional activity of the core RNA polymerase. During the course of our initial trials, we noted that control reactions lacking DNA template consistently yielded significant levels of ^{32}P-labeled RNA products; this robust and apparently DNA-independent RNA synthesis was observed only in the presence of RapA (Figure 2A, lane 4, red arrowheads). Sensitivity of the ^{32}P-labeled products to RNase (Figure 3A) and their insensitivity to proteinase K (data not shown) were consistent with RNA synthesis. This RNA-synthetic reaction could be carried out in the presence of excess (RNase-free) DNase (Figure 3B and Supporting Information Figure S1). RNA synthesis from ATP as a sole substrate and characteristic ladders resulting from the digestion of ^{32}P-labeled products by RNase (Figure 3A and Supporting Information Figure S1) clearly pointed to the synthesis of a polyriboadenylate. Quantitatively, the observed rates of polyriboadenylate synthesis from [α-^{32}P]ATP as a sole substrate

dx.doi.org/10.1021/bi101017x |*Biochemistry* 2011, 50, 2298–2312

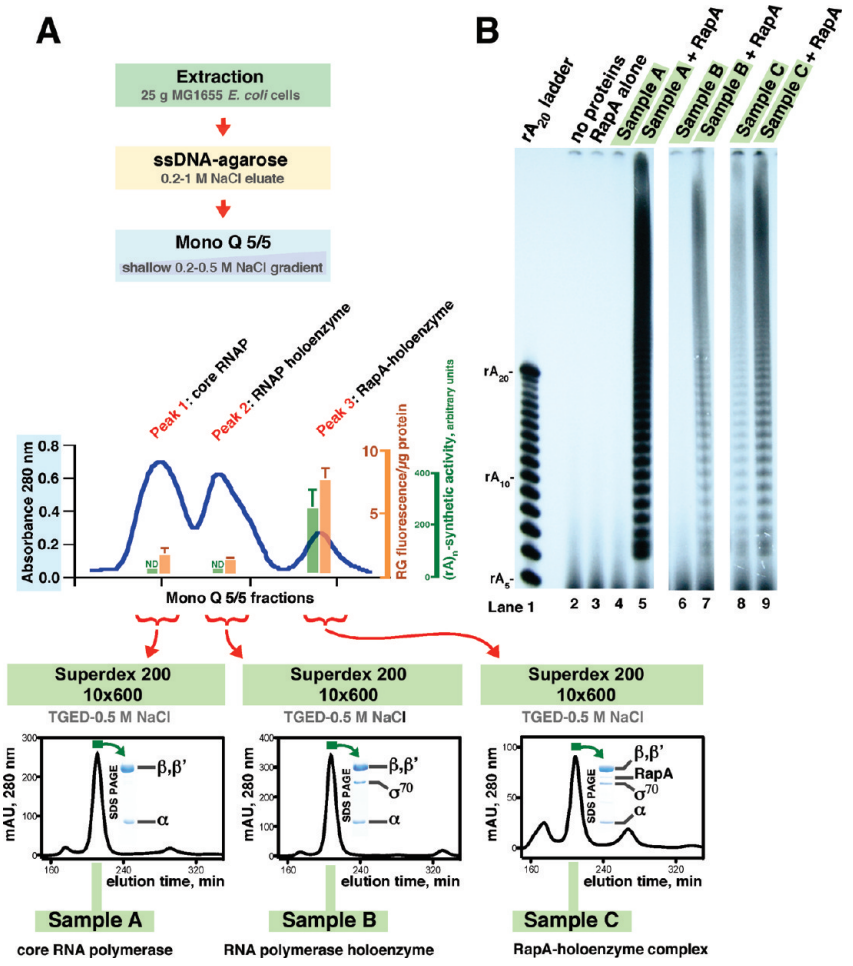

Figure 4. Poly(A)-synthetic activity is associated with the native RapA−RNA polymerase complex. (A) The core RNA polymerase, the RNA polymerase holoenzyme, and the native RapA−RNA polymerase holoenzyme complex were isolated as described in ref 7; a schematic of the purification procedure is shown in the left panel. At the Mono Q stage, $(rA)_n$-synthetic activity (bar graph, green columns) and nucleic acid content (bar graph, orange columns) in the fractions corresponding to the three forms of RNA polymerase were determined. $(rA)_n$-synthetic activity was assayed in buffer C, for 30 min at 37 °C, in the absence of RapA. The core RNA polymerase (peak 1), the RNA polymerase holoenzyme (peak 2), and the native RapA−RNA polymerase holoenzyme complex (peak 3), each 0.07 μM; [α-^{32}P]ATP, 0.14 mM. RiboGreen (RG) was used as a reporter of the fractions' nucleic acid contents. Fluorescent assays were carried out as described in Materials and Methods. Following the Mono Q stage, fractions containing the RNA polymerase species were pooled, concentrated, and subjected, individually, to an additional, gel-exclusion chromatography purification step in TGED buffer (see Materials and Methods) containing 0.5 M NaCl. The elution profiles (absorbance 280 nm *vs* time) are shown. Green bars indicate the peak fractions used for the enzymatic assay described in panel B; the inserts show the major peaks' protein content. (B) The purified core RNA polymerase (sample A), the RNA polymerase holoenzyme (sample B), and the native RapA−holoenzyme complex (sample C) were concentrated using Microcon Ultracel YM-30 centrifugal filters (Millipore) and assayed for an intrinsic $(rA)_n$-synthetic activity in buffer C, in the absence or in the presence of 0.4 μM wild-type (recombinant) RapA. The purified core RNA polymerase, the RNA polymerase holoenzyme, and the native RapA−holoenzyme complex, each 0.2 μM; [α-^{32}P]ATP, 0.14 mM. Note that the native RapA−holoenzyme complex obtained during the course of this purification procedure contained substoichiometric amounts of RapA (≤0.5 mol of RapA/mol of RNA polymerse) due to dissociation of a portion of RapA during the step of gel-exclusion chromatography (see Superdex 200 elution profile for the RapA−holoenzyme complex, peak at ~270 min). Reactions were incubated for 30 min at 37 °C and treated with DNase-free RNase as described in Figure 3A. Following the addition of an equal volume of stop solution (50% glycerol, 50 mM EDTA, 0.1% bromphenol blue, pH 7.5), the reaction mixtures were denatured by boiling, and ^{32}P-labeled reaction products were fractionated on 20% SequaGel. Note the lack of intrinsic $(rA)_n$-synthetic activity in the purified core RNA polymerase and the RNA polymerase holoenzyme (lanes 4 and 6) and an apparent $(rA)_n$-synthetic activity associated with the native RapA−RNA polymerase holoenzyme complex (lane 8).

were in the range of 4−11 pmol of [^{32}P]AMP incorporated into $(rA)_n$ per microgram of RapA per minute.

We questioned whether RapA's ATP-hydrolytic function is required for the RapA-dependent $(rA)_n$-synthetic reaction. To this end, we tested if and to what extent mutant RapA with an impaired ATP-hydrolytic function ($RapA^{R599A/Q602A}$)[7] would be able to promote the $(rA)_n$-synthetic reaction. Reactions with $RapA^{R599A/Q602A}$ showed significant (≥9-fold) reductions in the rates of $(rA)_n$ synthesis in comparison with reactions utilizing wild-type RapA (Figure 2A, compare lanes 5 and 6 to lanes 3 and 4; also Figure 2B, top panel) under otherwise similar conditions, suggesting a link between RapA's ATP hydrolytic function and its ability to switch "on" $(rA)_n$-synthetic activity in RapA−core RNA polymerase mixtures.

Because our RNA polymerase purification procedure, a derivative of the purification protocol developed by the Burgess group,[11]

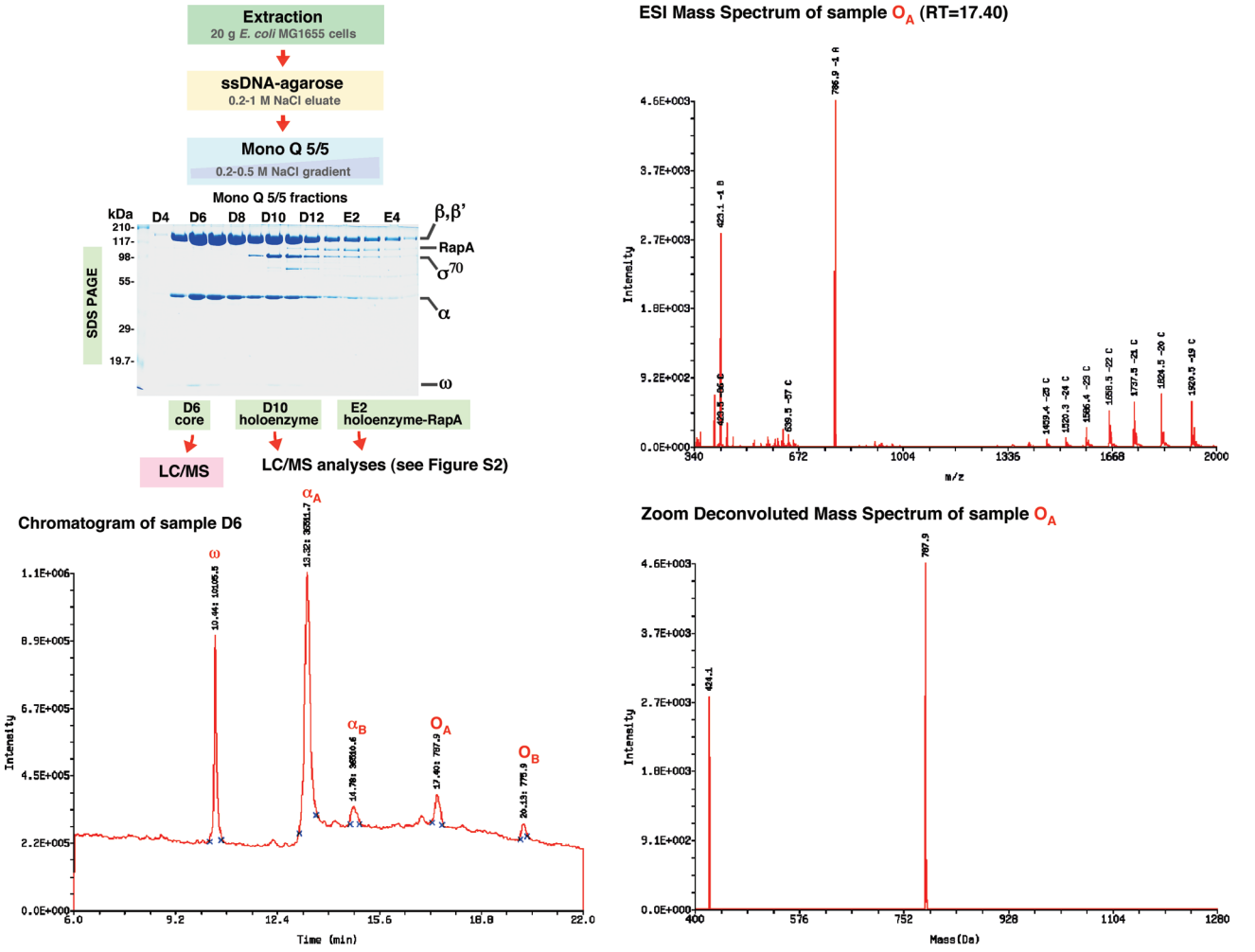

Figure 5. The *E. coli* RNA polymerase obtained through the classic purification procedure carries endogenous RNA oligonucleotides. The top panel shows a schematic for the purification of the native forms of the *E. coli* RNA polymerase. The protocol utilizing Mono Q chromatography for the separation of native RNA polymerase complexes was originally introduced by Hager *et al.*[11] This procedure was further developed in our studies.[3,7,8] The Mono Q fractions containing native RNA polymerase complexes (the core RNA polymerase, the RNA polymerase holoenzyme, and the holoenzyme−RapA complex[3]) are shown on a 12% SDS−polyacrylamide gel stained with EZBlue. The native RNA polymerase complexes were then subjected to LC/MS analyses. Panel below: 12.5 μL of the Mono Q fraction D6 (the core RNA polymerase) was injected onto a 2 × 50 mm ACE C18 column; LC was carried out as described in Supporting Information Figure S2. Each of the individual LC peaks was then subjected to mass spectrometry analyses. Representative mass spectra shown at the right correspond to the LC peak with the retention time of 17.4 min (peak O_A). Note that partition of these 787.9 Da species during the mass spectrometry stage yields 424.1 Da species (likely, adenosine diphosphate); the resulting difference in molecular mass is a match for guanosine monophosphate. For a complete set of mass spectra, see Supporting Information Figure S2.

yields three key forms of the RNA polymerase (core enzyme, holoenzyme, and the RapA−holoenzyme complex[3,8]), we measured $(rA)_n$-synthetic activities of the three forms of RNA polymerase obtained during the course of Mono Q chromatography (Figure 4). No apparent $(rA)_n$-synthetic activity was detected in fractions containing the core RNA polymerase and the RNA polymerase holoenzyme (Figure 4A, bar graph, green columns; also Figure 4B, lanes 4 and 6). In both cases, polyriboadenylate synthesis could be switched "on" by the addition of RapA (Figure 4B, lanes 5 and 7). In contrast, the native RapA−RNA polymerase complex showed measurable accessory $(rA)_n$-synthetic activity, as expected (Figure 4B, compare lane 8 with lanes 4 and 6; also Figure 4A, bar graph, green columns); this activity was enhanced when the reaction was supplemented with excess RapA (Figure 4B, lanes 8 and 9). Since our previous studies indicated that RapA could displace RNA polymerase-associated RNA,[7,9] we questioned whether native RapA−RNA polymerase complexes could contain an accessory nucleic acid. Analyses utilizing nucleic acid-specific fluorescent dyes (RiboGreen and SYBR II) yielded results consistent with either a greater amount of the accessory nucleic acid in the native RapA−RNA polymerase complexes or its greater accessibility to the fluorescent dyes [Figure 4A, bar graph (orange columns)].

Mechanistic Aspects of the RapA-Dependent Polyadenylation Reaction. We sought to extend our understanding of the mechanistic aspects of the observed $(rA)_n$-synthetic reaction and to determine whether the reaction represents a *de novo* $(rA)_n$ synthesis or the extension of an accessory, protein-associated nucleic acid fragment. To this aim, we analyzed the ^{32}P-labeled RNA products resulting from the RapA-dependent polyriboadenylation reaction on denaturing, high-percent polyacrylamide gels. During this set of experiments it became apparent that the observed $(rA)_n$-synthetic reaction relies exclusively on the extension of intrinsic, presumably core RNA polymerase-associated,

dx.doi.org/10.1021/bi101017x |*Biochemistry* 2011, 50, 2298–2312

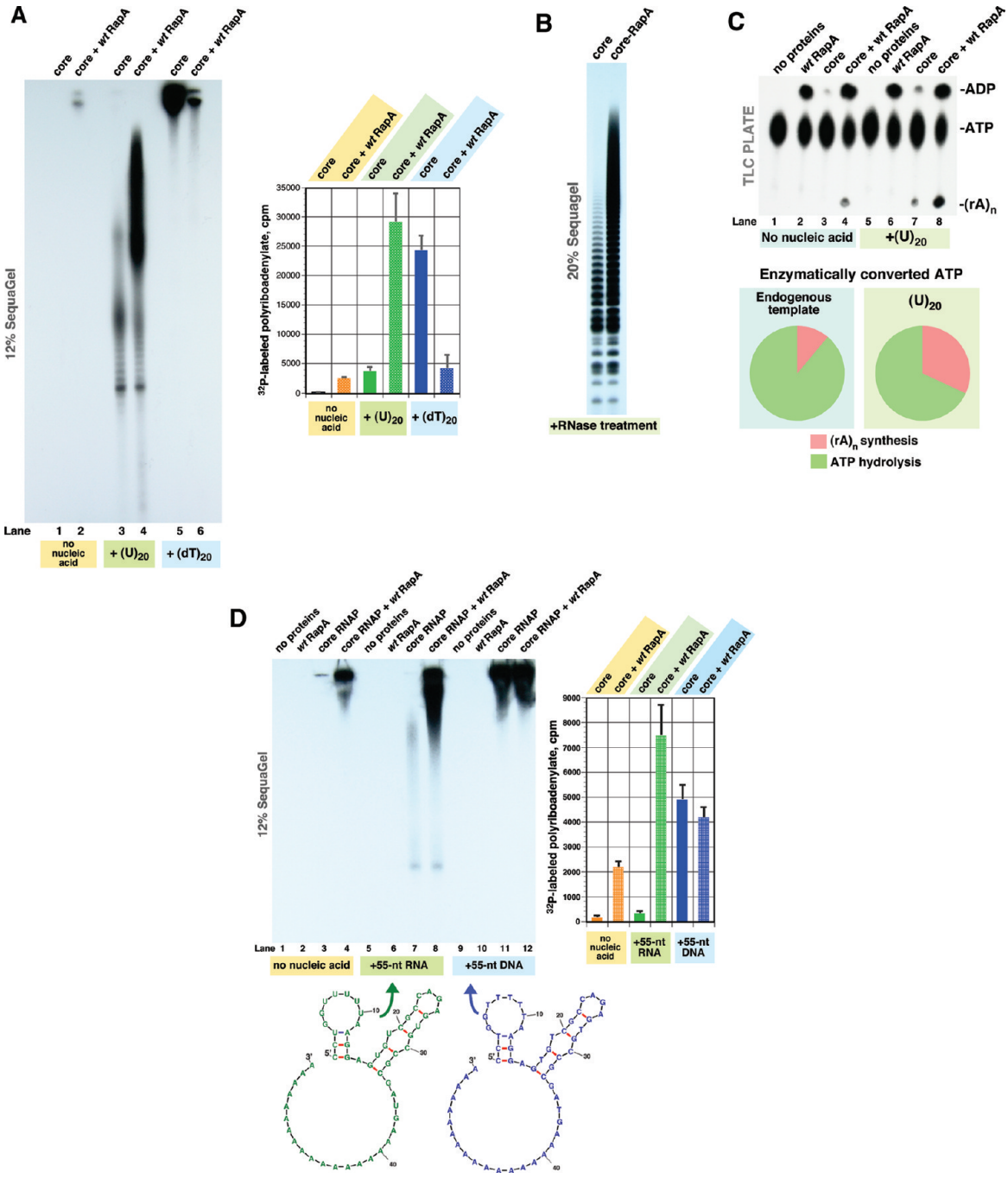

Figure 6. RapA-dependent polyadenylation of model, synthetic RNA templates. (A) RapA-dependent polyadenylation of $(U)_{20}$. Extension reactions in the absence (lanes 1 and 2) or presence of $(U)_{20}$ (lanes 3 and 4) or $(dT)_{20}$ (lanes 5 and 6) were carried out as described in Figure 3A for gel A. When indicated, $(U)_{20}$ or $(dT)_{20}$ was present at a final concentration of 0.29 μg/μL. The bar graph at the right shows the levels of total RNA in reactions carried out in the absence of nucleic acids (orange columns) or in the presence of $(U)_{20}$ (green columns) or $(dT)_{20}$ (blue columns). Data represent the average of two independent experiments. (B) Nuclease treatment of the extension products synthesized in RapA−core RNA polymerase−ATP mixtures in the presence of $(U)_{20}$. Gel-fractionated products of the reactions similar to those in lanes 3 and 4 in Figure 6A are shown, except that the reaction products were digested with DNase-free RNase; the RNase treatment was as described in Figure 3A. (C) Poly(rA)-synthetic and ATP-hydrolytic activity in RapA−core RNA polymerase−ATP mixtures in the presence of $(U)_{20}$. Reaction mixtures in lanes 1−4 were similar to those in lanes 1−4 in Figure 2A; lanes 5−8 show ATP-hydrolytic and poly(rA)-synthetic activity in the same reactions in the presence of 0.3 μg/μL $(U)_{20}$. Quantitative analysis of these data indicated that approximately 34% of enzymatically converted ATP was utilized for the poly(rA)-synthetic reaction (pie charts at the right). (D) RapA-dependent polyadenylation of a 55-nt RNA possessing a secondary structure. Extension reactions in the absence (lanes 1−4) or presence of 55-nt RNA (lane 5−8) or 55-nt DNA (lanes 9−12) were carried out as described in Figure 3A (gel A). When indicated, 55-nt RNA or 55-nt DNA was present at a final concentration of 0.3 μg/μL. The predicted secondary structures of 55-nt RNA and DNA probes are shown at the bottom. The bar graph at the right shows the levels of total RNA in reactions carried out in the absence of nucleic acids (orange columns) or in the presence of 55-nt RNA (green columns) or 55-nt DNA control (blue columns). Data represent the average of two independent experiments.

dx.doi.org/10.1021/bi101017x |*Biochemistry* 2011, 50, 2298–2312

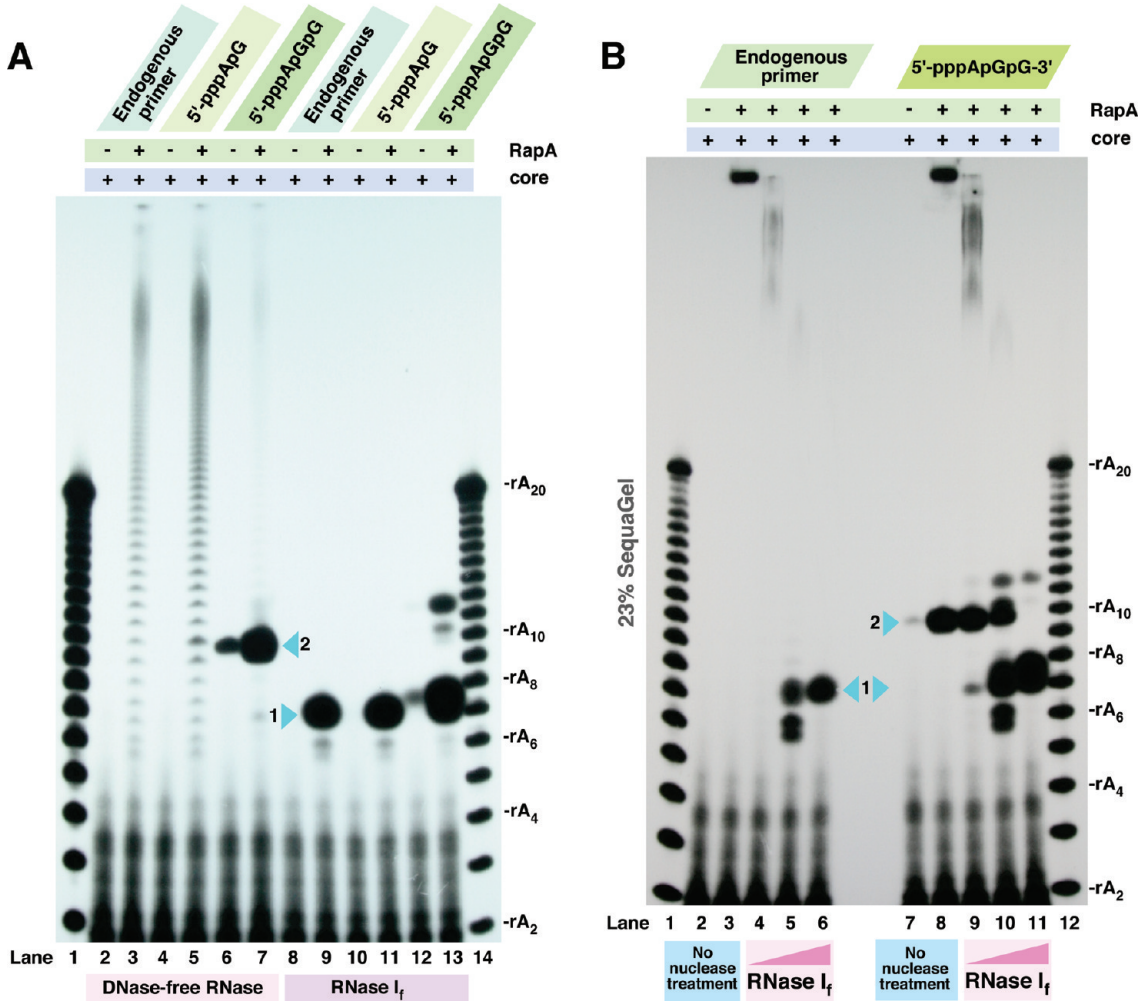

Figure 7. Effect of pppApG and pppApGpG on the RapA-dependent $(rA)_n$-synthetic reaction. Reactions were carried out in buffer C, as described in Materials and Methods. When indicated, the core RNA polymerase (isolated as described in Figure 4) was present at 0.19 μM; purified (recombinant, wild-type) RapA, at 0.45 μM; pppApG and pppApGpG (Dharmacon/Invitrogen), at 0.1 nmol/μL. In panel A, following a 30 min incubation at 37 °C, extension reactions were treated with either DNase-free RNase (Boehringer) (2 units/10 μL reaction) or RNase I_f (New England Biolabs) (10 units/10 μL reaction) for 5 min at room temperature before the addition of stop solution (see Materials and Methods). In panel B, products of reactions not treated with RNase (lanes 2, 3, 7, and 8) or reactions treated with 2 units/10 μL (lanes 4 and 9), 10 units/10 μL (lanes 5 and 10), or 50 units/10 μL (lanes 6 and 11) RNase I_f are shown. In both panels, RNase-resistant adducts (see Discussion and Supporting Information Figure S8) are highlighted with cyan arrowheads.

oligonucleotides. In Figure 3A, note a distinct lack of short (<6 nt long) ^{32}P-labeled RNAs in the nuclease digest of products synthesized in RapA−RNA polymerase mixtures (Figure 3A, gel B, lane 2) and their presence in the ^{32}P-labeled $(rA)_{20}$ control, which was treated with nuclease in a similar manner (Figure 3A, gel B, lanes 3 and 4). This result indicates that the extension products in question contain non-^{32}P-labeled oligonucleotide, presumably donated by the proteins. We next sought to confirm the identity of these oligonucleotide primers through liquid chromatography (LC)/mass spectrometry (MS) analyses. LC analyses of the native RNA polymerase complexes revealed a highly homogeneous class of small accessory molecules with molecular masses consistent with those of dinucleotides (775.9−787.9 Da) (Figure 5; also Supporting Information Figure S2). Partition of these dinucleotides during the MS stage yielded the differences in molecular masses matching that of guanosine monophosphate (Figure 5; also Supporting Information Figure S2B,D), an important result, pointing to the accessory nucleic acid fragments in question being the oligoribonucleotides. The remaining portion of the dinucleotide molecule (424.1 Da peaks in the mass spectra shown in Figure 5 and Supporting Information Figure S2B,D) showed a molecular mass consistent with that of ADP, the endogenous RNA dinucleotide thus likely being 5′-ppApG-3′. Because the aforementioned compounds were the only accessory nucleic acids detected by LC/MS analyses in purified native RapA−RNA polymerase complexes, which displayed apparent $(rA)_n$-synthetic activity (Figure 4), we concluded that these RNA polymerase-associated RNA fragments likely served as primers for RapA-dependent extension reactions. It is important to note that intrinsic RNA dinucleotides in preparations of the *E. coli* RNA polymerase have been previously reported. The functional significance of this association, however, is not fully understood.

Next, we tested whether model, synthetic RNA and DNA templates could be polyriboadenylated in a RapA-dependent manner. To this aim, we tested several dissimilar nucleic acid

templates, including $(U)_{20}$, $(dT)_{20}$, the 55-nt RNA possessing a secondary structure (shown schematically in Figure 6D), the 55-nt DNA probe with sequence matching (save U to T transitions) that of the 55-nt RNA as potential substrates for RapA-dependent polyriboadenylation. During the course of these experiments we determined that short synthetic RNAs served as good substrates for RapA-dependent extension reaction. As seen in Figure 6A, $(U)_{20}$ was efficiently extended in a largely RapA-dependent manner (Figure 6A, gel, lanes 3 and 4; Figure 6A, bar graph, green columns; also Figure 6B). With $(dT)_{20}$, RapA suppressed the synthesis of ^{32}P-labeled RNA (Figure 6A, graph, blue columns); overall, there was >30-fold difference in the amount of ^{32}P-labeled RNA resulting from switching from RNA to DNA for two oligonucleotides of the same length and similar base composition. With $(U)_{20}$, approximately 1 out of 3 enzymatically converted [α-^{32}P]ATP molecules in the reaction mixture was utilized for the polyriboadenylation reaction (Figure 6C, TLC plate, lane 8; also Figure 6C, pie charts). Extension assays with 55-nt RNA and DNA probes with similar base composition (save U to T transitions) consisting of a stem−loop structure at the 5′-terminus followed by an $(A)_{18}$ tail (Figure 6D, bottom panel) indicated a near-absolute requirement for RapA for RNA extension (Figure 6D, gel, lanes 7 and 8; also, bar graph, green columns). In contrast, with 55-nt DNA, the addition of RapA to the core RNA polymerase−[α-^{32}P]ATP−DNA mixtures led to a reduced synthesis of ^{32}P-labeled RNA (Figure 6D, graph, blue columns), in accord with the results of experiments described in Figure 6A. Taken together, these two sets of experiments point to RNA specificity of the RapA-dependent extension reaction.

Because our mass spectrometry analyses indicated that short RNA oligonucleotides copurified with native RNA polymerase complexes, we also carried out extension reactions in the presence or absence of synthetic RNA di- and trinucleotides [5′-pppApG-3′ and 5′-pppApGpG-3′ (Dharmacon)]. The addition of pppApG to *in vitro* extension reactions had little or no effect on the polyadenylation of endogenous RNA [in either Na^+/chloride- (Figure 7A, lanes 2−5) or K^+/acetate-based buffer system (Supporting Information Figure S3, lanes 2−5)]. In contrast, the addition of 5′-pppApGpG resulted in a robust extension reaction, which was accompanied by a synthesis of a ^{32}P-labeled, fixed-length product (Figure 7 and Supporting Information Figure S3, arrowhead 2).

Enzyme(s) Involved in RapA-Dependent Polyadenylation. We sought to determine whether $(rA)_n$ synthesis takes place in the active site of RNA polymerase, RapA, or an accessory protein, such as poly(A) polymerase (PAP) or polynucleotide phosphorylase (PNP), the two enzymes known to catalyze $(rA)_n$ synthesis in *E. coli*.[12,13] First, we subjected the core RNA polymerase (isolated as described in Figure 4) to an additional purification stage of gel-exclusion chromatography in high salt and compared its specific (RapA-dependent) $(rA)_n$-synthetic activity with that of the input material. There was no apparent loss of specific $(rA)_n$-synthetic activity in the core enzyme sample subjected to this additional purification step (Supporting Information Figure S4). Likewise, subjecting RapA to an additional, gel-exclusion chromatography purification step (in high salt) failed to alter its ability to switch "on" the $(rA)_n$-synthetic activity in the presence of the core RNA polymerase (data not shown).

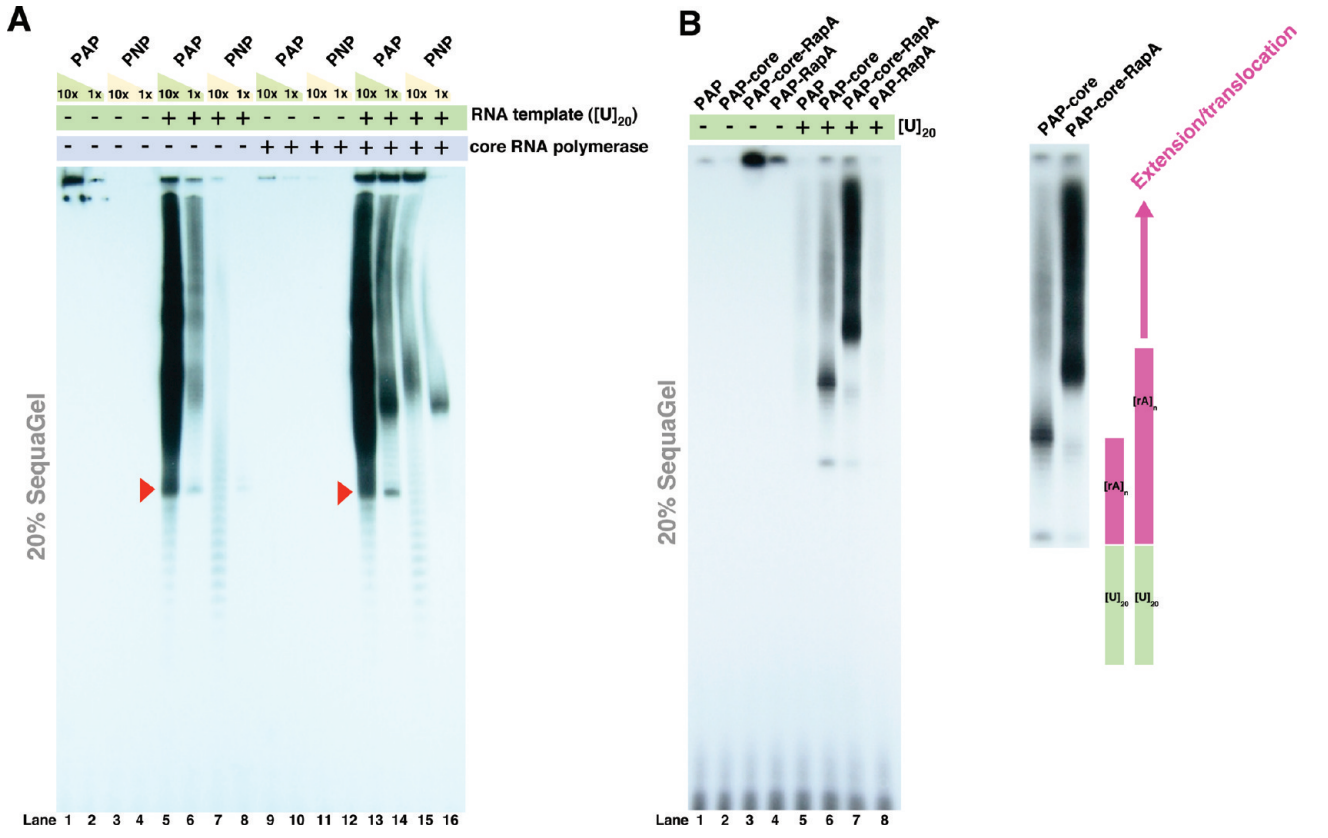

Figure 8. Continued

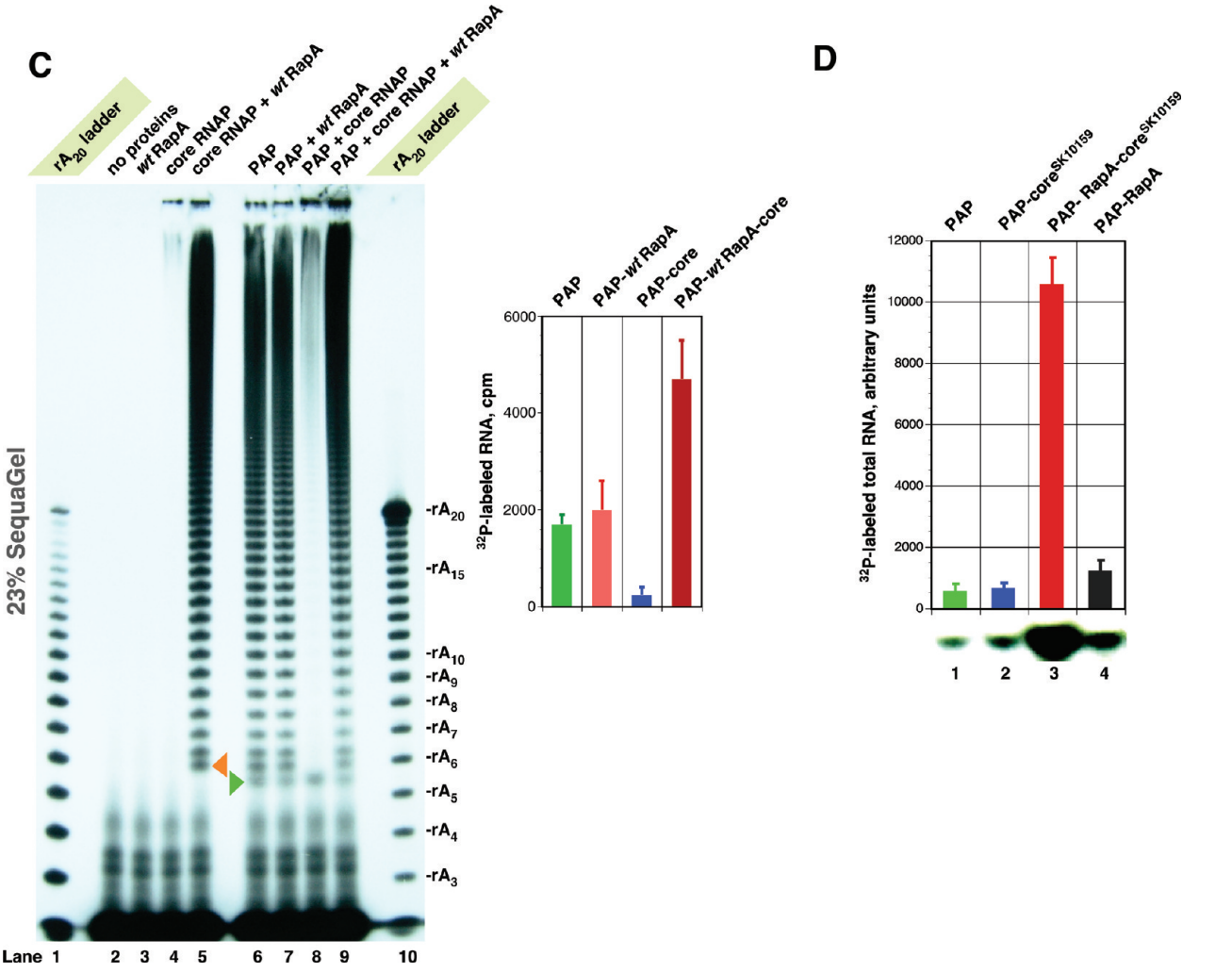

Figure 8. Polyadenylation of model, synthetic RNAs and endogenous oligonucleotides in reconstituted RNA polymerase−PAP and RNA polymerase−PNP model systems. (A) Polyadenylation of $(U)_{20}$ and endogenous oligonucleotides in a reconstituted RNA polymerase−PAP and RNA polymerase−PNP system: a side-by-side comparison of the extension products generated by PAP and PNP in the presence or absence of the core RNA polymerase. Reactions were carried out in buffer C (see Materials and Methods). When indicated, the purified core RNA polymerase (isolated as described in Figure 4) was present at 0.12 μM; $(U)_{20}$ (Dharmacon), at 0.2 μg/μL; PAP (PAP I; New England Biolabs), at either 0.5 unit/μL (10×) or 0.05 unit/μL (1×), and PNP (Sigma Aldrich), at either 0.1 unit/μL (10×) or 0.01 unit/μL (1×). Extension reactions were initiated by the addition of [α-^{32}P]ATP to the final concentration of 100 μM. After 30 min incubation at 37 °C, an equal amount of the stop solution (50% glycerol, 50 mM EDTA, 0.1% bromphenol blue, pH 7.5) was added to each 10 μL reaction. Samples were denatured by boiling for 1 min, and ^{32}P-labeled RNA products were analyzed on 20% SequaGel (National Diagnostics) using a Gibco BRL SA-type vertical electrophoresis apparatus. (B) Effect of RapA on PAP-mediated polyadenylation. Reactions were similar to those described in panel A, except that, when indicated, purified wild-type RapA was present at 0.41 μM. PAP I (New England Biolabs), 0.1 unit/μL. Schematic at the right: highlight of the results of the experiment. A similar experiment with PNP substituted for PAP is shown in Supporting Information Figure S7. (C) RapA-dependent polyadenylation of endogenous, protein-associated oligonucleotides in the presence or absence of PAP. Reactions were carried out in buffer C, as described in Materials and Methods. Reaction mixtures in lanes 2−5 were similar to those in lanes 1−4 in Figure 3A (gel A), except that the reaction products were treated with DNase-free RNase, as described in Figure 3A. Reaction mixtures in lanes 5−9 were similar to those in lanes 1−4, except that each reaction contained 0.25 unit/μL *E. coli* PAP (New England Biolabs). The quantitated levels of total RNA in reactions 6−9 are shown at the right. Green and orange arrowheads indicate the shortest ^{32}P-labeled extension products synthesized in the presence or absence of PAP. Note that the observed differences in length are likely due to PAP-mediated extension of endogenous, RNA polymerase-associated and PAP-associated primers. (D) RapA enables PAP-mediated polyadenylation of RNA polymerase-associated RNA. Reactions were similar to those in lanes 5−8 in panel B, except that the core RNA polymerase (isolated as described in Figure 4) was substituted with the core RNA polymerase isolated from the PAP$^-$ PNP$^-$ *E. coli* strain (core^{SK10159}) (see Supporting Information Figure S5). The bar graph shows the levels of total ^{32}P-labeled RNA in reactions containing PAP (lane 1), PAP plus core^{SK10159} (lane 2), PAP plus core ^{SK10159} plus RapA (lane 3), and PAP plus RapA (lane 4).

Next, we tested if the RNA polymerase's accessory, RapA-dependent $(rA)_n$-synthetic activity is sensitive to the RNA polymerase inhibitor rifampicin. These experiments indicated little or no effect of rifampicin on RapA-dependent polyadenylation (data not shown), the result arguing against the direct involvement of RNA polymerase in the extension reaction in question.

We then obtained the *E. coli* strain carrying the PAP and PNP deletion mutations (see Materials and Methods) and purified the core RNA polymerase from this strain, using our recently

dx.doi.org/10.1021/bi101017x |*Biochemistry* 2011, 50, 2298–2312

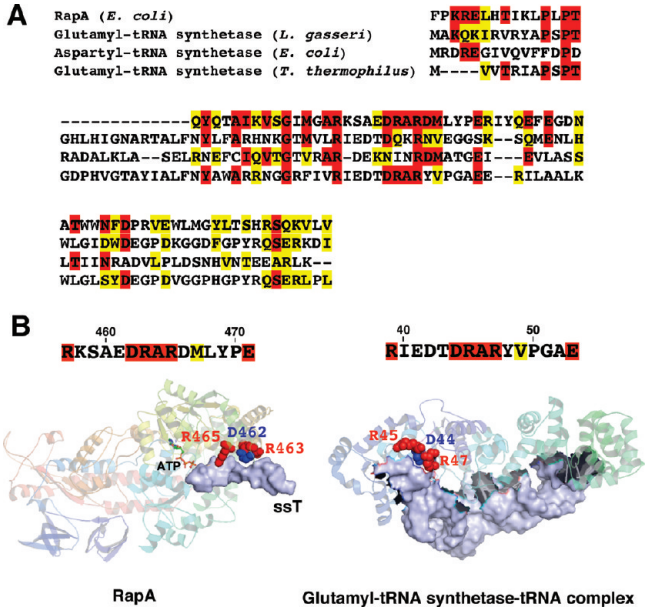

Figure 9. RapA's SWI/SNF domain carries motifs found in enzymes with established functions in modification of the 3′-termini of ssRNA. (A) Alignments demonstrating partial sequence homology between RapA and bacterial aspartyl- and glutamyl-tRNA synthetases. Identical and homologous amino acids are highlighted with red and yellow boxes. Panel B shows a model of the RapA−ssT complex[7,10] side-by-side with that of the *T. thermophilus* glutamyl-tRNA synthetase−tRNA complex.[23] The polar amino acids in the conserved "DRAR" clusters (which, in both proteins, engage single-stranded nucleic acid near its 3′-terminus) are shown as red and blue spheres.

developed small-scale RNA polymerase purification procedure (Supporting Information Figure S5). The core RNA polymerase obtained from the PAP/PNP-deficient strain displayed no detectable accessory $(rA)_n$-synthetic activity (Supporting Information Figure S5), an important result pointing toward an accessory enzyme, such as PAP or PNP likely carrying out the actual polymerization step.

We next sought to reconstitute the transcription complexes possessing $(rA)_n$-synthetic activity from purified components. To this aim, we obtained the purified *E. coli* PAP and PNP (see Materials and Methods) and compared $(rA)_n$-synthetic activities of the two enzymes in the presence or absence of purified RNA polymerase and/or RNA. These analyses produced results consistent with the RNA polymerase-associated $(rA)_n$-synthetic activity being due to an accessory PAP (Figure 8). In side-by-side comparisons, patterns of the extension products seen in RNA polymerase−PAP mixtures mimicked those seen in RapA-dependent polyadenylation reactions described in Figure 6. For example, note a distinct extension product containing the first ^{32}P-labeled base added to the $(U)_{20}$ template (Figure 8A, red arrowheads; also Figure 8B; compare this extension pattern with that seen in Figure 6A, lanes 3 and 4). This pattern was not seen with PNP. Also, PNP displayed a characteristic nuclease activity in addition to its poly(A)-synthetic activity (Supporting Information Figure S7), a known property of this enzyme.[13] In the RNA polymerase−(purified) PAP model system, the addition of RapA resulted in distinctly longer extension products [Figure 8B; note that the presence of the polymerase was essential for the efficient extension of $(U)_{20}$ under these conditions (compare lanes 5, 6, and 7)]. With PAP, in the absence of exogenous RNA templates and RNA polymerase, some $(rA)_n$ synthesis was detected (Figure 8C, lane 6), possibly due to a trace of endogenous RNA priming the extension reaction. Mixing PAP with the core RNA polymerase resulted in a near-complete shutdown of PAP's $(rA)_n$-synthetic activity (Figure 8C, gel, compare lanes 6 and 8; also Figure 8C, graph). Addition of purified RapA to the PAP−core enzyme mixture fully reversed this repression and stimulated (by 3−5-fold) the polyadenylation reaction (Figure 8C, gel, lanes 8 and 9; also Figure 8C, graph). Thus, in the reconstituted PAP−RNA polymerase system, the polyadenylation of an endogenous primer also could be switched "on" by RapA (Figure 8C, lanes 8 and 9). With the "PAP-free" core RNA polymerase [isolated from the PAP-deficient *E. coli* strain (Supporting Information Figure S5)], it was also possible to mimic the RapA-dependent polyadenylation reaction in reconstituted RapA−core RNA polymerase−(purified) PAP mixtures (Figure 8D). Finally, we have confirmed the presence of PAP in our RNA polymerase preparations through immunoassays with PAP-specific polyclonal antibodies (Supporting Information Figure S6).

Based on these analyses, we have concluded that our results are consistent with RapA enabling the polyadenylation of endogenous, protein-associated RNA fragments by PAP.

RapA's Domains Involved in Interaction with RNA. Because these results, along with the results of our two preceding studies,[7,9] suggested that RapA could remodel RNA polymerase−RNA complexes, we questioned whether RapA's SWI/SNF domain, specifically, its section linked to interaction with a single-stranded nucleic acid,[7,10] shared homology with enzymes known to selectively bind and remodel RNA. These comparative analyses have determined that RapA's SWI/SNF domain contained motifs found in bacterial aspartyl- and glutamyl-tRNA synthetases (Figure 9). While there was limited structural homology between RapA and tRNA synthetases in general, the single-stranded nucleic acid recognition motifs involved in interaction with RNA's 3′-terminus (including the most conserved "R----DRAR" amino acid clusters) were virtually identical in the two proteins (Figure 9; there was approximately 40% homology between the aligned segments of RapA and *Thermus thermophilus* glutamyl-tRNA synthetase shown in Figure 9A).

Because both sequence and structure homology analyses pointed to the same cluster of amino acids within RapA's SWI/SNF domain as a potential single-stranded nucleic acid-(RNA-) binding site (Figure 10A, top panel, amino acids shown as red, blue, and green spheres), we sought to mutate selected amino acids within this cluster in order to test how such mutations would affect RapA's abilty to enable $(rA)_n$ synthesis in the RNA polymerase−(accessory) PAP system. To this aim, we chose to remodel the conserved "RKSAEDRAR" cluster in RapA by replacing some of the polar amino acids (R465, E461, and the R457/K458 pair) with substitutions of opposite charge (Figure 10A, bottom panel). The mutant RapA (referred hereafter as RapA*) was constructed and purified in a manner similar to that described for wild-type RapA (Figure 10B). Interestingly, RapA* eluted as two distinct peaks during the Source Q chromatography (Figure 10B shows the Source Q profiles for wild-type RapA and RapA* resulting from two parallel purifications of similar scale); this elution pattern was not seen with any of the previously constructed RapA mutants.[7] We probed the Source Q fractions resulting from these two protein purifications (of wild-type RapA and RapA*) with nucleic acid-specific fluorescent dyes and have determined that the second peak in RapA*'s Source Q fractions

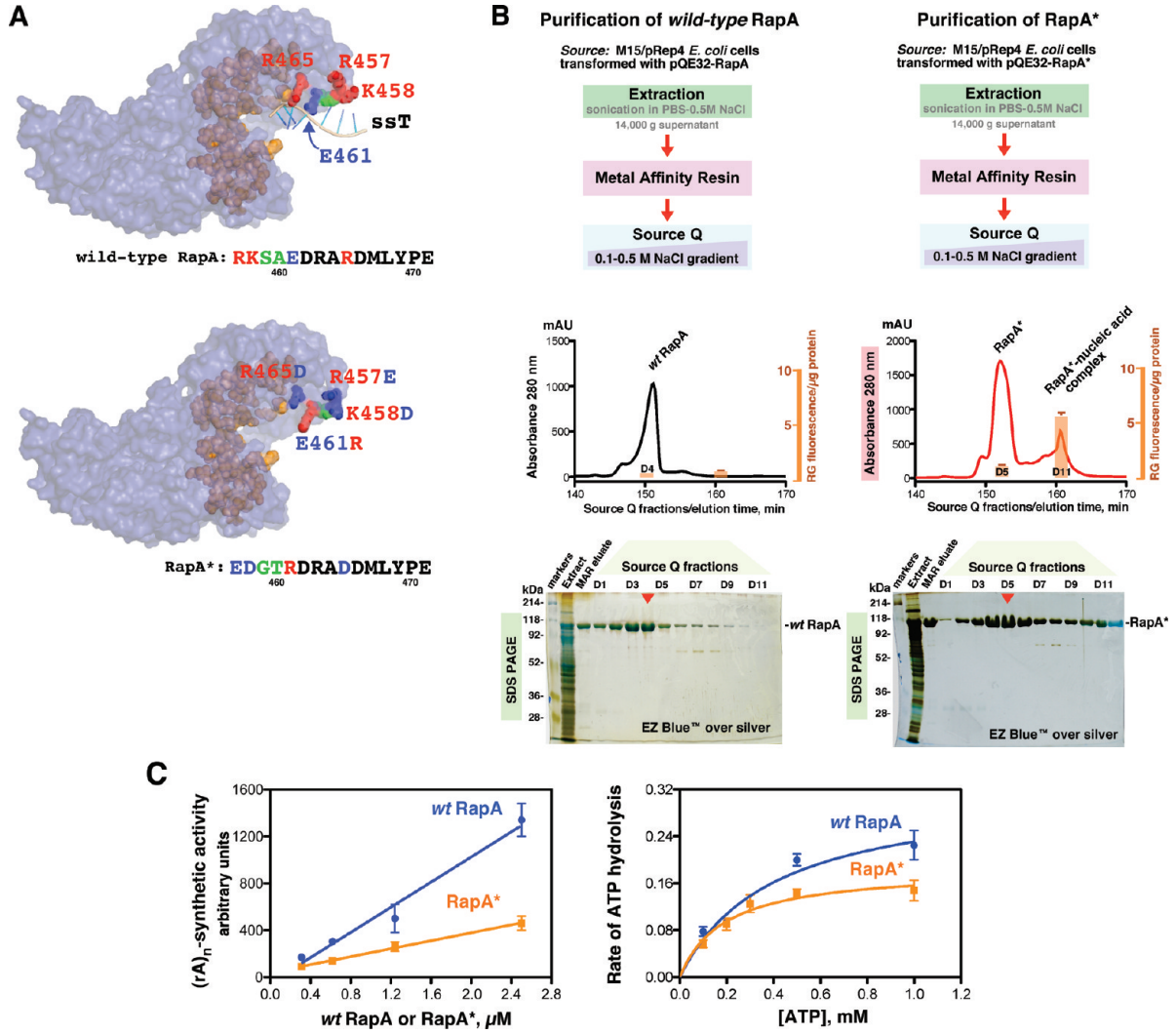

Figure 10. Mutations in RapA's SWI/SNF domain alter RapA's nucleic acid-binding activity and $(rA)_n$-synthetic activity of the RapA−core RNA polymerase complex. (A) A model of the wild-type RapA−ssT complex[7,10] is shown in the top panel. The target amino acids are highlighted as red, green, and blue spheres. The structure of RapA* is shown at the bottom. In both panels, consensus amino acids in RapA's SWI/SNF motifs[1,2] are shown as orange and brown spheres. (B) Schematics for the purification of recombinant, His-tagged wild-type RapA (panels at the left) and RapA* (panels at the right). The fractions from the final purification steps (Source Q column) are shown below on denaturing polyacrylamide gels stained with EZBlue (Sigma-Aldrich) over silver. The red arrowheads indicate the RapA peak fractions used in the experiments described below. The bar graphs on Source Q elution profiles show the nucleic acid content of the fractions determined in fluorescent assays with RG (see Materials and Methods). (C) Poly(A)-synthetic activity in RapA−core RNA polymerase−(accessory) PAP mixtures as a function of RapA concentration. Extension reactions with recombinant wild-type RapA (blue circles) and RapA* (orange rectangles) were similar to those described in Figure 2, except that the concentration of the core RNA polymerase (containing endogenous PAP) was 0.76 μM and [α-^{32}P]ATP, 0.18 mM. Bottom panel: Effect of the RapA* mutation on RapA's ATP-hydrolytic activity; rate of ATP hydrolysis [mM ATP hydrolyzed in 30 min reactions containing 0.94 μg of purified wild-type RapA (blue circles) or RapA* (orange rectangles) per 16 μL reaction] is plotted as a function of ATP concentration. ATP-hydrolytic activity assays and data analyses were similar to those described in ref 7 (see Figure 2D therein), except that the reactions were carried out in buffer C (see Materials and Methods).

(which eluted at higher salt concentration) contained protein-associated nucleic acid (Figure 10B, bar graph). We next tested the effect of the constructed mutation on RapA-dependent polyadenylation. Side-by-side comparisons of RapA* with wild-type RapA indicated a moderate, 2−3-fold reduction of the initial rates of polyadenylate production with the former protein under otherwise similar conditions (Figure 10C). In contrast, the ATP-hydrolytic activity of RapA* ($K_{m,ATP}$ and V_{max} for ATP hydrolysis) was largely comparable to that of wild-type RapA; there was a <1.4-fold reduction in V_{max} for ATP hydrolysis resulting from the mutation in question (Figure 10C); the mild effect of this mutation on ATP hydrolysis was expected and consistent with the location of the mutation site on the side of RapA's SWI/SNF domain opposite to that facing the ATP cleft.

In vitro extension assays with synthetic RNA primers (such as pppApGpG) also confirmed the reduced ability of RapA* to enable the polyadenylation of RNA in comparison to that of wild-type RapA (Figure 11).

Contribution of RapA to RNA Polyadenylation *in Vivo*. We questioned whether RapA could make a measurable contribution to RNA polyadenylation *in vivo*. To test this, we labeled nucleic acids in *E. coli* MG1655*rapA*$^+$ and MG1655*rapA*$^-$ cells with ^{32}P *in vivo* and compared the amounts of ^{32}P-labeled nucleic acids [obtained through two independent, dissimilar extraction methods

dx.doi.org/10.1021/bi101017x |*Biochemistry* 2011, 50, 2298–2312

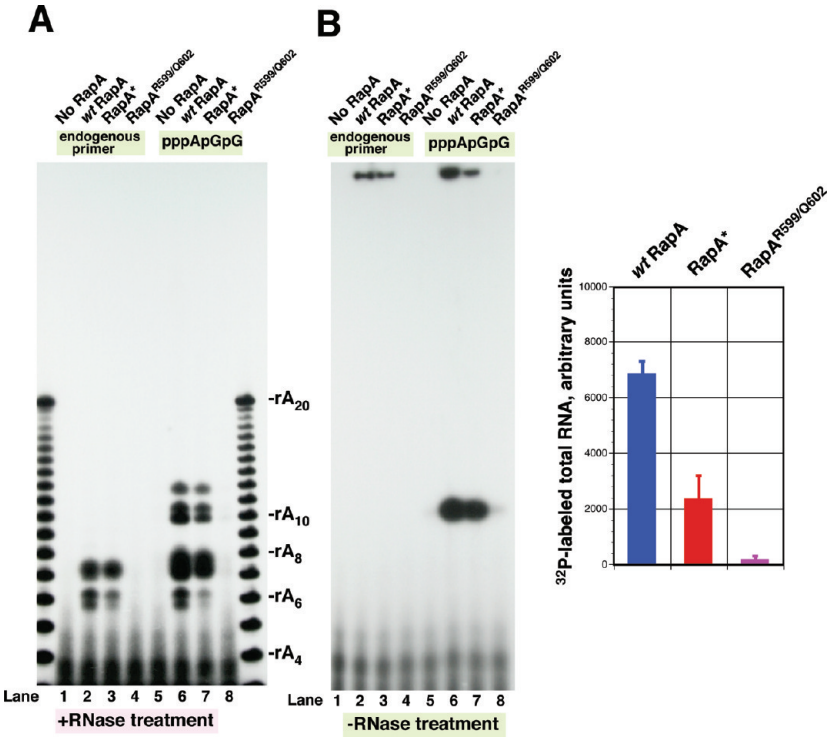

Figure 11. Effect of the mutations in RapA's SWI/SNF domains on polyadenylation of endogenous, RNA polymerase-associated and synthetic RNA primers. Reactions were carried out in buffer C, as described in Materials and Methods. When indicated, recombinant, wild-type RapA, RapA*, and RapA$^{R599A/Q602A}$ [7] were present at approximately 0.4 μM; the core RNA polymerase (isolated as described in Figure 4 and containing endogenous PAP), at 0.22 μM; and pppApGpG (Dharmacon/Invitrogen), at 0.1 nmol/μL. Panel A: Reaction mixtures were treated with RNase I$_f$ (New England Biolabs), as described in Figure 7A. Panel B: Similar to panel A, except that the nuclease treatment of reaction mixtures was omitted. The bar graph shows the levels of total ^{32}P-labeled RNA in reactions containing the synthetic RNA primer (pppApGpG).

(see Materials and Methods)] retained on oligo(dT) DNA-cellulose cartridges. The results of this set of experiments are shown in Figure 12. As seen in Figure 12, there was a consistent reduction in the amount of ^{32}P-labeled material retained on oligo(dT) DNA-cellulose cartridges from the *rapA*$^-$ *E. coli* strain (Figure 12, bar graphs), independent from the extraction method.

■ DISCUSSION

In this work, we demonstrate that RapA, the auxiliary SWI/SNF subunit of the *E. coli* RNA polymerase,[3−10] modulates the polyadenylation of endogenous, RNA polymerase-associated RNA primers and model, synthetic RNA templates. We demonstrate that $(rA)_n$-synthetic activity copurifies with the *E. coli* RNA polymerase. (i) Insensitivity of this accessory activity to rifampicin, (ii) its loss in RNA polymerase isolated from the PAP-deficient *E. coli* strain, (iii) our ability to mimic the observed reaction in reconstituted RapA−RNA polymerase−(purified) PAP mixtures, and (iv) physical presence of accessory PAP in RNA polymerase preparations suggest that RapA enables the polyadenylation by PAP of endogenous, RNA polymerase-associated RNA. Mass spectrometry analyses identified such an accessory, endogenous RNA in native RNA polymerase complexes (Figure 5; also Supporting Information Figure S2). Small accessory RNA oligonucleotides have been known to copurify with the *E. coli* RNA polymerase; their origin is often linked to RNA polymerase's "stuttering" synthesis. The RNA polymerase-associated RNA fragments in question were integral to all three native forms of RNA polymerase (the core RNA polymerase, RNA polymerase holoenzyme, and the holoenzyme−RapA complex). The 5′-termini of these oligonucleotides were unavailable to a T4 PNK-mediated exchange reaction (data not shown); their 3′-termini could not be efficiently extended by PAP (in the absence of RapA). In LC/MS experiments, elution of these endogenous RNA species from C18 matrix-bound RNA polymerase subassembly components was observed at denaturing conditions. All three lines of evidence point to the RNA oligonucleotides in question being deeply embedded in protein and tightly bound. Thus, other hypotheses regarding their origin (such as the nuclease processing of nonproductive transcription complexes with the extruded RNA's 3′ end[14,15]) or their potential roles as integral nucleic acid cofactor species cannot be ruled out. The ability of RapA to enable the polyadenylation of endogenous RNAs suggests a function for RapA in remodeling of RNA polymerase−RNA complexes. It seems likely that this remodeling could amount to ATP-dependent extraction or translocation of RNA polymerase-associated RNA (Figure 13), since the mutations disrupting RapA's ATP-hydrolytic function also greatly diminished this activity. Such a function would be consistent with the results of our recent studies, which pointed to RNA as RapA's primary nucleic acid substrate.[7,9] It also would be in accord with the established role of RapA as an integral element of the apparatus for RNA synthesis in *E. coli*,[3−7] particularly taking into account the established role of RapA in remodeling of nonproductive transcription complexes.[6] Currently unresolved issues include understanding the exact mode of attachment of the poly(A) tail to the endogenous RNA primers. Our analyses point to the possibility of phosphate−phosphate

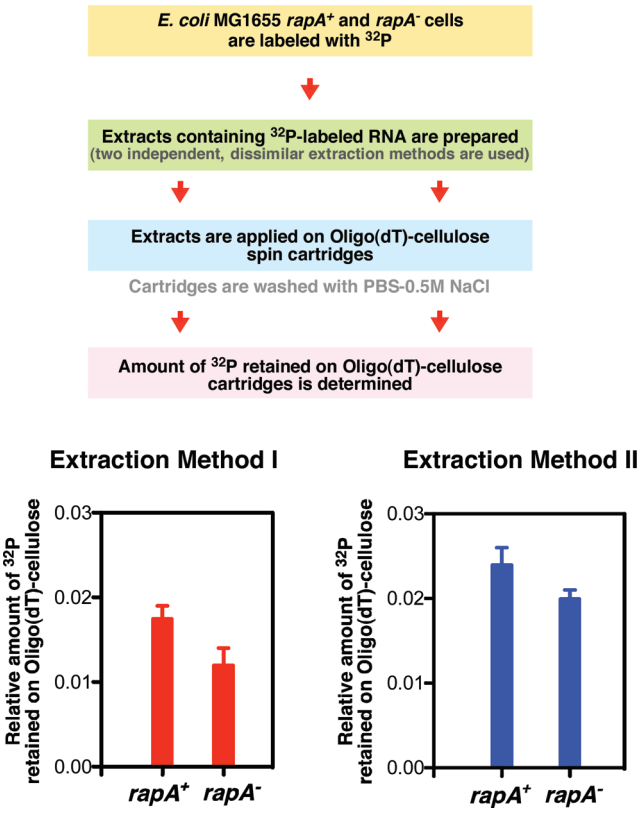

Figure 12. RapA contributes to RNA polyadenylation *in vivo*. A schematic above illustrates the design for this set of experiments. *in vivo* ^{32}P labeling was carried out as described in Materials and Methods. Quantitated results of two independent sets of experiments are shown below. The extraction method I included a lysozyme treatment and multiple cycles of freezing and thawing; in the extraction method II, cells were treated with a nonionic detergent.

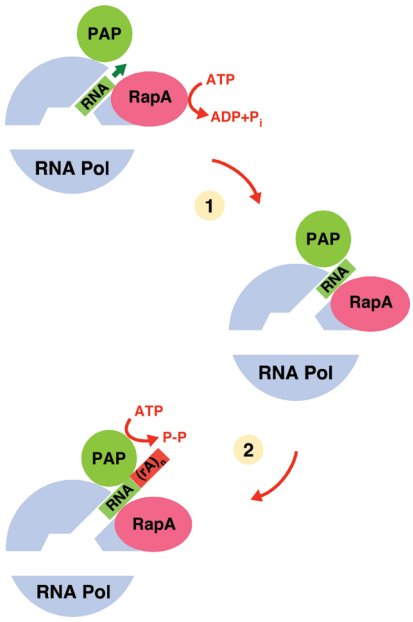

Figure 13. RapA enables the polyadenylation by PAP of RNA polymerase-associated RNA. A model for the function of RapA described in this work. Stage 1: RapA extracts/translocates the core RNA polymerase-associated RNA. Stage 2: RNA is polyadenylated by an accessory PAP. Note that this mechanism could apply to the complexes with extruded RNAs 3′ end.[14] A model for the polyadenylation of endogenous RNA fragments with extruded 5′ end is shown in Supporting Information Figure S8.

bonds in the primer−poly(A) tail junction region (Figure 8C, orange and green arrowheads). Because a conventional positioning of the endogenous RNA in the RNA polymerase's active site, with its 5′-terminus facing RapA/PAP, would make its extension impossible, an alternative mechanism could involve the formation of a functional 3′-OH group through a modification of the endogenous RNA primer's 5′ end with ATP (Supporting Information Figure S8). To test this hypothesis, we digested the products in question (resulting from extension of either endogenous, RNA polymerase-associated primer or synthetic RNA trinucleotide) with RNase I_f. (RNase I_f, a derivative of RNase I, cleaves at ssRNA nucleotide−phosphate−nucleotide bonds leaving a 5′-hydroxyl and a 3′-linked monophosphate.) In accord with the proposed mechanism, under all experimental conditions and with dissimilar types of primers, these experiments demonstrated the formation of largely RNase I_f-resistant adducts [Figure 7 and Supporting Information Figure S3 (cyan arrowheads); also Supporting Information Figure S8].

In this work we demonstrate the polyadenylation of model, synthetic RNA templates in a RapA-dependent manner (Figures 6 and 7). Note that with some of these templates [such as the 55-nt RNA incorporating a stem−loop structure followed by an $(rA)_{18}$ tail at the 3′ end, for example] there was a near-absolute requirement for RapA for RNA extension (Figure 6D, lanes 7 and 8). The development of these enzymatic assays is particularly important for future studies with RapA due to an obvious ambiguity in discriminating between the effects of RapA on RNA and DNA during *in vitro* transcription and *in vivo* studies.[6,7] In a reconstituted RNA polymerase−PAP model system, RNA polymerase suppressed the PAP-mediated polyadenylation of endogenous RNAs. RapA fully reversed this effect and further boosted the PAP-mediated extension reaction (Figure 8C). The addition of RapA to the core RNA polymerase−PAP mixtures resulted in a synthesis of distinctly longer extension products (Figure 8B). RapA also enhanced the polyadenylation of $(U)_{20}$ by PNP in the presence or absence of RNA polymerase (Supporting Information Figure S7). Functional significance of these effects remains to be elucidated.

Our work suggests that RapA's SWI/SNF domain may be involved in interaction with RNA. Mutations in this domain (specifically, in the cluster of amino acids previously linked through homology modeling to interaction with a single-stranded nucleic acid)[7,9] moderately altered RapA-dependent polyadenylation. Comparative analyses reveal similar motifs in aspartyl- and glutamyl-tRNA synthetases, a well-characterized class of enzymes. In tRNA synthetases, the motifs in question are responsible for binding of the portion of the tRNA molecule near its 3′ end (Figure 9, bottom panels).

SWI/SNF proteins likely have evolved from (ancient precursors to) the DEAD/H family of DNA and RNA helicases, and it is generally established that their function is related to nucleic acid management. Their distinctive feature, a "SWI/SNF" domain (representing an extension of the DEAD/H helicase domain IV), implies a shared general function and, arguably, a functional complexity beyond that found in DEAD/H family of DNA and RNA helicases. Recent views about such shared function have coalesced around the idea of their translocation on dsDNA.[16−18] Our previous studies have linked RapA, the prokaryotic

representative of SWI/SNF family, to RNA remodeling.[7,9] We hypothesized that RapA could function in remodeling of ssRNA−RNA polymerase and ssRNA−dsDNA complexes.[7,9] This work provides further proof that the function of RapA is linked to remodeling of RNA−RNA polymerase complexes. The data presented in this study are consistent with RapA acting as an ATP-dependent RNA translocase. Our data indicate that this activity of RapA may be functionally significant (Figure 12). The ability of RapA to act as an RNA polymerase-associated extractor of RNA "jammed" in RNA polymerase's active site could have accounted for the previously reported transcription-stimulatory activity of RapA.[6] The RapA's RNA translocase function is also consistent with the reported functions of its eukaryotic counterparts,[16−18] with an important substitution of RNA for DNA.

■ ASSOCIATED CONTENT

Supporting Information. Eight additional figures and methods. This material is available free of charge via the Internet at http://pubs.acs.org.

■ AUTHOR INFORMATION

Corresponding Author

*E-mail: msoukhodol@my.lamar.edu. Phone: 409-880-7905 (office); 409-880-7906 (laboratory). Fax: 409-880-8270.

Funding Sources

This work was supported in part by Grant R15GM081803 from the National Institute of General Medical Sciences (to M.V.S.) (the content of this study is solely the responsibility of the authors and does not necessarily represent the official views of the National Institute of General Medical Sciences or the National Institutes of Health), a Welch Foundation grant (V-0004), and departmental funds.

■ ACKNOWLEDGMENT

We thank S. K. Kushner (University of Georgia, Athens) for providing the PAP$^-$ PNP$^-$ *E. coli* strain, A. J. Carpousis (CNRS, Toulouse, France) for PAP-specific antibodies, and Mark E. Hail (Novatia) for technical assistance with mass spectrometry analyses.

■ ABBREVIATIONS

ADP, adenosine 5′-diphosphate; ATP, adenosine 5′-triphosphate; BSA, bovine serum albumin; EDTA, ethylenediaminetetraacetic acid; LC, liquid chromatography; MS, mass spectrometry; PAP, poly(A) polymerase; PNP, polynucleotide phosphorylase; PAGE, polyacrylamide gel electrophoresis; PEI, polyethylenimine; RG, RiboGreen; RNAP, RNA polymerase; SDS, sodium dodecyl sulfate; ss, single-stranded; TBE, Tris−borate−EDTA; TLC, thin-layer chromatography; UV, ultraviolet.

■ REFERENCES

(1) Bork, P., and Koonin, E. V. (1993) An expanding family of helicases within the "DEAD/H" superfamily. *Nucleic Acids Res. 21*, 751–752.

(2) Kolstø, A. B., Bork, P., Kvaløy, K., Lindback, T., Grønstadt, A., Kristensen, T., and Sander, C. (1993) Prokaryotic members of a new family of putative helicases with similarity to transcription activator SNF2. *J. Mol. Biol. 230*, 684–688.

(3) Sukhodolets, M. V., and Jin, D. (1998) RapA, a novel RNA polymerase-associated protein, is a bacterial homolog of SWI2/SNF2. *J. Biol. Chem. 273*, 7018–7023.

(4) Sukhodolets, M. V., and Jin, D. (2000) Interaction between RNA polymerase and RapA, a bacterial homolog of SWI2/SNF2. *J. Biol. Chem. 275*, 22090–22097.

(5) Muzzin, O., Campbell, E. A., Xia, L., Severinova, E., Darst, S. A., and Severinov, K. (1998) Disruption of *Escherichia coli* hepA, an RNA polymerase-associated protein, causes UV-sensitivity. *J. Biol. Chem. 273*, 15157–15161.

(6) Sukhodolets, M. V., Cabrera, J. E., Zhi, H., and Jin, D. J. (2001) RapA, a bacterial homolog of SWI2/SNF2, stimulates RNA polymerase recycling in transcription. *Genes Dev. 15*, 3300–3341.

(7) Yawn, B., Zhang, L., Mura, C., and Sukhodolets, M. V. (2009) RapA, the SWI/SNF subunit of *Escherichia coli* RNA polymerase, promotes the release of nascent RNA from transcription complexes. *Biochemistry 48*, 7794–7806.

(8) Sukhodolets, M. V., Garges, S., and Jin, D. J. (2003) Purification and activity assays of RapA, the RNA polymerase-associated homolog of the SWI/SNF superfamily. *Methods Enzymol. 370*, 283–290.

(9) McKinley, B. A., and Sukhodolets, M. V. (2007) *Escherichia coli* RNA polymerase-associated SWI/SNF protein RapA: evidence for RNA-directed binding and remodeling activity. *Nucleic Acids Res. 35*, 7044–7060.

(10) Shaw, G., Gan, J., Zhou, Y. N., Zhi, H., Subburaman, P., Zhang, R., Joachimiak, A., Jin, D., and Ji, X. (2008) Structure of RapA, a SWI2/SNF2 protein that recycles RNA polymerase during transcription. *Structure 16*, 1417–1427.

(11) Hager, D. A., Jin, D. J., and Burgess, R. R. (1990) Use of Mono Q high-resolution ion-exchange chromatography to obtain highly pure and active *Escherichia coli* RNA polymerase. *Biochemistry 29*, 7890–7894.

(12) Sarkar, N. (1997) Polyadenylation of mRNA in prokaryotes. *Annu. Rev. Biochem. 66*, 173–197.

(13) Mohanty, B. K., and Kushner, S. R. (2000) Polynucleotide phosphorylase functions both as a 3′→5′ exonuclease and a poly(A) polymerase in *Escherichia coli*. *Proc. Natl. Acad. Sci. U.S.A. 97*, 11966–11971.

(14) Komissarova, N., and Kashlev, M. (1997) Transcriptional arrest: *Escherichia coli* RNA polymerase translocates backward, leaving the 3′ end of the RNA intact and extruded. *Proc. Natl. Acad. Sci. U.S.A. 94*, 1755–1760.

(15) Nudler, E., Mustaev, A., Lukhtanov, E., and Goldfarb, A. (1997) The RNA-DNA hybrid maintains the register of transcription by preventing backtracking of RNA polymerase. *Cell 89*, 33–41.

(16) Nimonkar, A. V., Amitani, I., Baskin, R. J., and Kowalczykowski, S. C. (2007) Single molecule imaging of Tid1/Rdh54, a Rad54 homolog that translocates on duplex DNA and can disrupt joint molecules. *J. Biol. Chem. 282*, 30776–30784.

(17) Amitani, I., Baskin, R. J., and Kowalczykowski, S. C. (2006) Visualization of Rad54, a chromatin remodeling protein, translocating on single DNA molecules. *Mol. Cell 23*, 143–148.

(18) Prasad, T. K., Robertson, R. B., Visnapuu, M. L., Chi, P., Sung, P., and Greene, E. C. (2007) A DNA-translocating Snf2 molecular motor: *Saccharomyces cerevisiae* Rdh54 displays processive translocation and extrudes DNA loops. *J. Mol. Biol. 369*, 940–953.

(19) Sukhodolets, M. V., and Garges, S. (2003) Interaction of *Escherichia coli* RNA polymerase with the ribosomal protein S1 and the Sm-like ATPase Hfq. *Biochemistry 42*, 8022–8034.

(20) Cao, G., and Sarkar, N. (1992) Identification of the gene for an *Escherichia coli* poly(A) polymerase. *Proc. Natl. Acad. Sci. U.S.A. 89*, 10380–10384.

(21) Thomä, N. H., Czyzewski, B. K., Alexeev, A. A., Mazin, A. V., Kowalczykowski, S. C., and Pavletich, N. P. (2005) Structure of the SWI2/SNF2 chromatin-remodeling domain of eukaryotic Rad54. *Nat. Struct. Mol. Biol. 12*, 350–356.

(22) Eisen, J. A., Sweder, K. S., and Hanawalt, P. C. (1995) Evolution of the SNF2 family of proteins: subfamilies with distinct sequences and functions. *Nucleic Acids Res. 23*, 2715–2723.

(23) Sekine, S., Nureki, O., Dubois, D. Y., Bernier, S., Chenevert, R., Lapointe, J., Vassylyev, D. G., and Yokoyama, S. (2003) ATP binding by glutamyl-tRNA synthetase is switched to the productive mode by tRNA binding. *EMBO J. 22*, 676–688.